ORGANOMETALLICS

Article

pubs.acs.org/Organometallics

Synthesis, Structures, and Dynamic Features of d^0 Zirconocene–Allyl Complexes

Mihaela Vatamanu

Department of Chemistry, Queen's University, Kingston, Ontario K7L 3N6, Canada

ABSTRACT: The reaction of $[Cp_2ZrMe][MeB(C_6F_5)_3]$ (**1**) with 2,4-dimethyl-1-pentene and 2,4-dimethyl-1-heptene, respectively, in C_6D_5Cl at 25 °C results in irreversible formation of the cationic Cp_2Zr^+–allyl complexes $[Cp_2Zr(\eta^3\text{-}CH_2C(CH_2R)\text{-}CH_2)]^+$ (**2a**, **3a**) and $[Cp_2Zr(\eta^3\text{-}CH_2C(Me)CHR)]^+$ (**2b**, **3b**) (**2a,b**, R = $CH(CH_3)_2$; **3a,b**, R = $CH(CH_3)CH_2CH_2CH_3$) and release of methane. The Cp_2Zr^+–allyl complexes were characterized with regard to their structures and rearrangement dynamics of their allyl ligands by NMR spectroscopy. Variable-temperature ^1H NMR experiments show that the allyl ligands of complexes **2a,b** and **3a,b** are fluxional. The fluxional behavior in these complexes is mainly due to a mechanism that involves η^3 to η^1 isomerization, rotation of the allyl carbon–carbon π unit about the carbon–carbon σ bond, and reversion to the η^3-allyl coordination mode, when both the allyl syn/anti hydrogen exchange and apparent Cp ligand exchange occur. The rotation of the C=C unit about the allyl carbon–carbon σ bond also results in a reversal of the η^3-allyl coordination face relative to the Cp_2Zr^+ moiety. A second mechanism which may account for the apparent Cp ligand exchange in the Cp_2Zr^+–allyl complexes under investigation consists of rotation of the η^3-coordinated allyl ligand about the metal–allyl bond. The free energy of activation for the exchange processes, as estimated from the coalescence temperature of the two Cp ligands, is between 54 and 60 kJ/mol. Aside from the intramolecular allyl exchange processes described above, this study also shows that the η^1- and η^3-coordinated allyl forms of a particular Zr–allyl complex coexist in solution and that the equilibrium composition of these species is temperature dependent. The Cp_2Zr^+–allyl complexes described in this paper serve as models for similar cationic Cp_2Zr^+–allyl intermediates implicated in zirconocene-catalyzed alkene polymerization reactions.

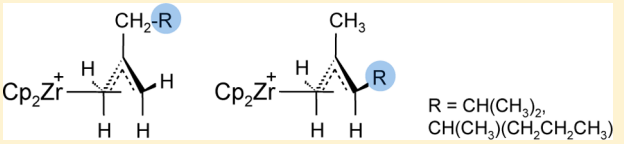

INTRODUCTION

In recent years there has been considerable research in the use of metallocene complexes of the type $[Cp'_2ZrR]^+[X]^-$ (Cp′ = substituted η^5-cyclopentadienyl type ligand, R = alkyl group, X^- = weakly coordinating anion) as homogeneous catalysts for alkene polymerization.[1] Extensive research conducted in this area has tremendously advanced the mechanistic understanding of the general processes involved in the initiation, propagation, chain transfer, and termination steps, such that many details regarding the polymerization mechanism seem to be reasonably well understood.[1]

Of special interest lately, however, is the observation that most of the metallocene catalysts, although very reactive at the beginning of the polymerization, are affected adversely by a number of side reactions which lead to a gradual decrease in catalyst activity, and therefore productivity.[2] In spite of extensive research to date, the underlying mechanisms responsible for catalyst deactivation are still poorly understood.[3] Although part of the catalyst can be irreversibly deactivated due to ubiquitous impurities in the catalytic system, or as a result of decomposition at high temperatures,[3b] a large fraction of the catalyst seems to be reversibly deactivated, or in a "dormant" state, as inferred from the observation that the catalyst activity increases when the polymerization is run in the presence of a small amount of H_2.[4]

A mechanism that has been advanced to explain the hydrogen activation effect[4] invokes a reactivation of Zr–polymeryl species arising from 2,1-insertion of propene. For steric reasons, these species are assumed to be slow to propagate and hence to accumulate in the polymerization system.[5] So far, however, all attempts to detect secondary Zr–polymeryl intermediates during catalysis have failed[6] and their existence has only been implied from analyses of polymer microstructures[7] and end groups.[8] Moreover, in a recent study, Liu et al.[9] have found that a secondary Zr–butyl compound was not particularly inert to insertion of propene and, thus, the subject remains controversial.[6a,10]

A few reports also suggested that the hydrogen activation effect can be the result of the hydrogenolysis of Zr–allyl species, also proposed to arise during alkene polymerization and remain in a "dormant" state.[11] A general reaction path suggested to account for the formation of cationic Zr–allyl species during propene polymerization is shown in eq 1. Here,

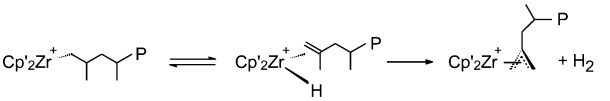

(1)

the cationic zirconium hydride alkene complex $[Cp'_2Zr(H)(CH_2{=}C(Me)CH_2CH(Me)P)]^+$ (P = long-chain alkyl or polymeryl group; the counterion $[X]^-$ has been omitted for simplicity), generated via β-hydride elimination of the Zr–

Received: October 6, 2013

dx.doi.org/10.1021/om400972u | *Organometallics* XXXX, XXX, XXX–XXX

polymeryl intermediate $[Cp'_2Zr\text{-}CH_2CH(Me)CH_2CH(Me)\text{-}P]^+$, transfers an allylic hydrogen atom from the coordinated vinylidene-terminated polymer chain to the hydride ligand to form the cationic Zr–allyl species $[Cp'_2Zr(\eta^3\text{-}CH_2C(CH_2CH(Me)P)CH_2)]^+$ along with a dihydrogen molecule.[3b,12]

Alternatively, the vinylidene-terminated polymer chain released in solution following the β-hydride elimination reaction can recoordinate to the active catalyst $[Cp'_2Zr\text{-}R]^+$ (R = H, Me, polymeryl chain) to form the $[Cp'_2Zr(R)(CH_2{=}C(Me)CH_2CH(Me)P)]^+$ intermediate. This again can transfer an allylic hydrogen atom from the coordinated vinylidene-terminated polymer chain to the R ligand to give a cationic Zr–allyl species and release an RH molecule (eq 2).[13,14]

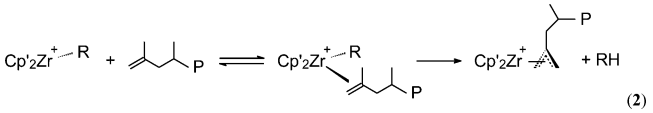

(2)

In contrast to the hydrogenolysis of secondary Zr–polymeryl species which can be easily detected by analyzing the ^{13}C NMR spectra of the saturated end groups of the polymer chains,[4] the reaction of Zr–allyl species with molecular hydrogen would result in polymers with unsaturated end groups similar to those arising from other chain termination processes. Thus, while a significant amount of catalyst could be trapped as Zr–allyl species during polymerization, the hydrogen activation effect as a result of hydrogenolysis of these species can be overlooked.

The formation of Zr–allyl species during alkene polymerization reactions is generally inferred from the detection of internal unsaturation on the polymer chain[8b,15] and the observation of dihydrogen gas released during the polymerization.[16] Recently, however, the presence of Zr–allyl intermediates in a polymerization mixture could be observed directly by the use of in situ NMR spectroscopic studies. Thus, Al-Humydi et al.[13] have noted formation of oligomeric Zr–allyl complexes of the type $Me_2C(Cp)(indenyl)Zr^+(\eta^3\text{-}CH_2C(P)CH_2)$ (P = $-(CH_2CH(Me))_nC_3H_7$) as byproducts in propene polymerization by $[Me_2C(Cp)(indenyl)Zr(Me)][MeB(C_6F_5)_3]$, while Landis and Christianson[12] identified two diastereomeric forms of the cationic Zr–allyl species (SBI)$Zr^+(\eta^3\text{-}CH_2C(P)CHCH_2CH_2CH_3)$ (SBI = *rac*-$Me_2Si(indenyl)_2$ and P = $-(CH_2C(C_4H_9))_nCH_2SiMe_3$), while performing low-temperature NMR studies on 1-^{13}C-1-hexene polymerization catalyzed by $[(SBI)ZrCH_2SiMe_3)][B(C_6F_5)_4]$. These observations are of fundamental interest. Since the dominant chain termination process in alkene polymerization involves β-H elimination reactions with formation of cationic Cp'_2Zr^+–H and release of unsaturated terminated polymer chains,[1] the formation of Zr–allyl complexes from either the cationic $Cp'_2Zr^+(H)(alkene)$ (eq 1) or a cationic zirconium alkene intermediate of the general type $Cp'_2Zr^+(R)(alkene)$ (eq 2) might be quite general. Therefore, understanding the structures, bonding, and solution behavior of Zr–allyl intermediates, or models thereof, is becoming increasingly important.

Several examples of cationic Zr–allyl complexes containing unsubstituted or Me-substituted allyl ligands, examples of which include $(C_5H_4Me)_2Zr^+(\eta^3\text{-}C_3H_5)(THF)$,[17a] $(C_5Me_5)_2Zr^+(\eta^3\text{-}C_3H_5)$,[17b] $(SBI)Zr^+(\eta^3\text{-}2\text{-}Me\text{-}C_3H_4)$,[12] $Me_2C(Cp)(indenyl)\text{-}Zr^+(\eta^3\text{-}2\text{-}Me\text{-}C_3H_4)$,[13] and $Cp'_2Zr^+(\eta^3\text{-}2\text{-}Me\text{-}C_3H_4)$, where Cp′ = C_5H_5, C_5Me_5, $C_5H_4C(Me_3)$,[18] were synthesized and characterized. In all of these complexes, the allyl ligand was found to have η^3 coordination relative to the metal center and display fluxional behavior.

Surprisingly, only a few cationic Zr–allyl complexes of the general type $Cp'_2Zr^+(\eta^3\text{-}CH_2C(R)CH_2)$ or $Cp'_2Zr^+(\eta^3\text{-}CH_2C(Me)CHR)$, where R = ethyl or longer alkyl chain, have been reported and little is known about the structures and dynamics of these complexes. For instance, Al-Humydi et al.[13] reported the synthesis of $[Me_2C(Cp)(indenyl)Zr(\eta^3\text{-}CH_2C(CH_2CMe_3)CH_2)]^+$ from the reaction of 2,4,4-trimethyl-1-pentene with $[Me_2C(Cp)(indenyl)Zr{-}Me]^+$, while Horton[18a] noted the formation of cationic Zr–allyl complexes from the reactions of 2-methyl-1-butene, 2-methyl-1-pentene, and 2-ethyl-1-butene, respectively, with $[Cp_2ZrMe]^+$. However, detailed structural characterization of these complexes seems to be lacking. Also, no information on the dynamics of these complexes has been provided.

Recently, we have investigated the in situ reaction of $[Cp_2ZrMe][B(C_6F_5)_4]$ with 2,4-dimethyl-1-pentene in C_6D_5Cl.[14] The study established that $[Cp_2ZrMe]^+$ does react with 2,4-dimethyl-1-pentene to form methane and an allyl complex, $[Cp_2Zr(\eta^3\text{-}CH_2C(CH_2CHMe_2)CH_2)]^+$, and that the reaction occurs via the $[Cp_2Zr(Me)(CH_2{=}C(Me)\text{-}CH_2CHMe_2)]^+$ intermediate (see eq 2), which was observed by low-temperature one- and two-dimensional ^1H NMR spectroscopy. In this paper, the results of a detailed experimental study on the synthesis, spectroscopic characterization, and dynamic behavior of a series of cationic Cp_2Zr^+–allyl complexes obtained from the reaction of $[Cp_2ZrMe][MeB(C_6F_5)_3]$[19] with 2,4-dimethyl-1-pentene and 2,4-dimethyl-1-heptene, respectively, in C_6D_5Cl at ambient temperature are reported. These complexes serve as models for cationic Cp_2Zr^+–allyl intermediates implicated in zirconocene-catalyzed alkene polymerization reactions.

RESULTS AND DISCUSSION

Reaction of $[Cp_2ZrMe][MeB(C_6F_5)_3]$ with 2,4-Dimethyl-1-pentene. Addition of 1.5 equiv of 2,4-dimethyl-1-pentene to a C_6D_5Cl solution of $[Cp_2ZrMe][MeB(C_6F_5)_3]$ (**1**), generated in situ by reacting Cp_2ZrMe_2[20a,b] with 1.1 equiv of $B(C_6F_5)_3$[20c] at ambient temperature, resulted in a slow color change of the reaction mixture from yellow to orange-brown. Monitoring by ^1H NMR spectroscopy revealed that the reaction proceeds slowly, being complete within 8 h. When 5 equiv of 2,4-dimethyl-1-pentene was used, the reaction was complete in less than 3 h. The reaction of **1** with 2,4-dimethyl-1-pentene is expected to proceed as in Scheme 1, where the two cationic Zr–allyl complexes $[Cp_2Zr(\eta^3\text{-}CH_2C(CH_2CHMe_2)CH_2)]^+$ (**2a**) and $[Cp_2Zr(\eta^3\text{-}CH_2C(Me)CHCHMe_2)]^+$ (**2b**) can form along with methane.

During the course of the reaction, the *Cp* and Zr–*Me* resonances of **1** at δ 5.97 (s) and 0.56 (s), respectively, and the 2,4-dimethyl-1-pentene[21] resonances all decreased in intensity. At the same time, the *Me*–B resonance of **1** at δ 0.34 (br s) first broadened and then narrowed and shifted downfield toward a

Scheme 1

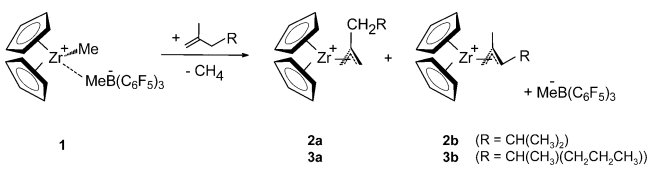

1 **2a** **3a** **2b** (R = $CH(CH_3)_2$) **3b** (R = $CH(CH_3)(CH_2CH_2CH_3)$)

dx.doi.org/10.1021/om400972u | *Organometallics* XXXX, XXX, XXX–XXX

Table 1. NMR[a] Data of the η^3-Allyl Unit in Complexes 2a,b and 3a,b

compd	assignt	^{1}H	^{13}C
$Cp_2Zr^+(\eta^3\text{-}CH_2C(CH_2R)CH_2)$ (**2a**)	CH_2	2.54 (s, H_s, 2H), 3.36 (s, H_a, 2H)	67.2 ($^1J_{CHs}$ = 159, $^1J_{CHa}$ = 145)
	C		162
$Cp_2Zr^+(\eta^3\text{-}CH_2C(Me)CHR)$ (**2b**)	CH_2		70
	CH	4.1	92 ($^1J_{CH}$ = 143)
	C		159
$Cp_2Zr^+(\eta^3\text{-}CH_2C(Me)CHR)$ (**2b**)[b]	CH_2	2.32 (d, J_{HH} = 1.9, H_s), 3.29 (d, J_{HH} = 1.9, H_a)	
	CH	3.75 (d, J_{HH} = 9.4)	
$Cp_2Zr^+(\eta^3\text{-}CH_2C(CH_2R)CH_2)$ (**3a**)	CH_2	2.58 (s, H_s), 3.42 (s, H_a)	68 ($^1J_{CHs}$ = 159, $^1J_{CHa}$ = 145)
	CH_2	2.56 (s, H_s), 3.36 (s, H_a)	67 ($^1J_{CHs}$ = 159, $^1J_{CHa}$ = 145)
	C		162
$Cp_2Zr^+(\eta^3\text{-}CH_2C(Me)CHR)$ (**3b**)	CH_2	1.85 (H_s), 3.0 (d, $^2J_{HH}$ = 4.5, H_a)	57 ($^1J_{CHs}$ = 157, $^1J_{CHa}$ = 149)
	CH	4.6 (d, $^3J_{HH}$ = 9.1, H_a)	106 ($^1J_{CH}$ = 137)
	C		158

[a]The NMR (600 MHz) spectra were acquired in chlorobenzene-d_5 at 0 °C unless otherwise noted. Chemical shifts are given in ppm; coupling constants are reported in Hz. R = $CHMe_2$ (**2a,b**), $CH(Me)CH_2CH_2CH_3$ (**3a,b**). [b]The ^{1}H NMR spectrum was acquired at −40 °C. The complete assignments are detailed in the Experimental Section.

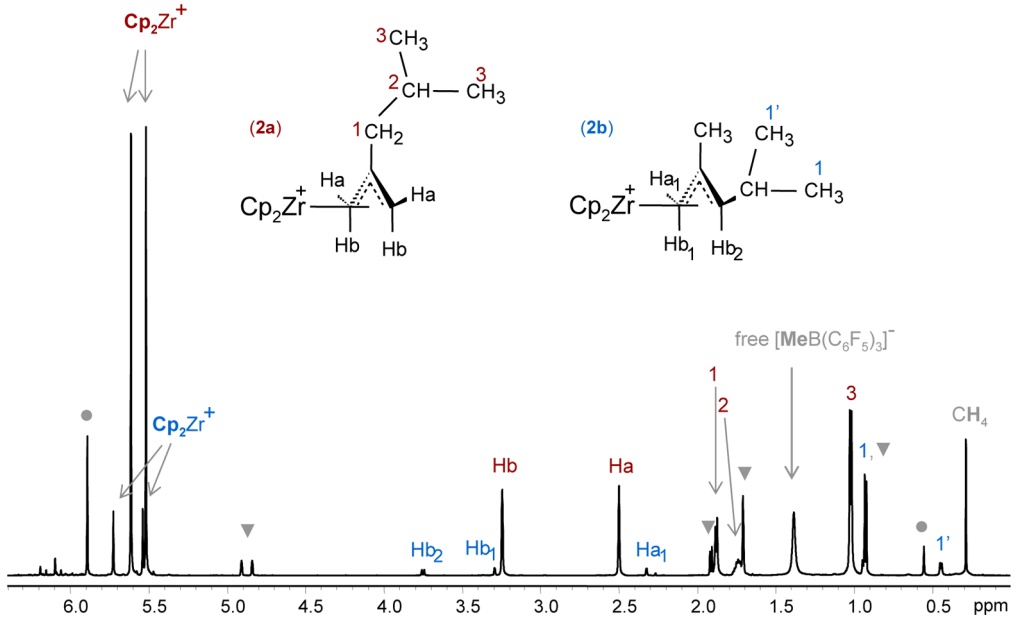

Figure 1. ^{1}H NMR spectrum of the in situ reaction between $[Cp_2ZrMe][MeB(C_6F_5)_3]$ and 2,4-dimethyl-1-pentene (1:1 mole ratio) in C_6D_5Cl (600 MHz, −40 °C): (●) $[Cp_2ZrMe]^+$; (▼) 2,4-dimethyl-1-pentene.

free $[MeB(C_6F_5)_3]^-$ position. Note that at ambient temperature the ^{1}H NMR *Me*−B resonance in the free $[MeB(C_6F_5)_3]^-$ anion appears at δ 1.16, as determined by the reaction of **1** with acetonitrile-d_3 (1:3 mole ratio) in C_6D_5Cl (see the Experimental Section).[22] Moreover, a series of new resonances at δ 5.70 (br s), 3.47 (s), 2.56 (s), 1.99 (d), and 0.98 (d) also appeared in addition to the anticipated resonance of methane observed at δ 0.25. The integration ratio of the resonances at δ 5.70, 3.47, and 2.56 is 10:2:2. On this basis, and in consideration of previous reports on related complexes,[18a,b] these resonances were attributed to the Cp (δ 5.70) and CH_2 (δ 3.47 and 2.56) allyl hydrogens of **2a**. In addition, the resonances at δ 1.99 and 0.98 were attributed to the methylene and methyl hydrogens of the $-CH_2CHMe_2$ group, respectively; the methyne resonance of the $-CH_2CHMe_2$ group could not be observed due to overlap with the analogous methyne resonance of unreacted 2,4-dimethyl-1-pentene at δ 1.77.

To confirm the above assignments and gain further information about the structural features of **2a**, the sample was cooled to 0 °C and further analyzed by ^{1}H NMR and correlation spectroscopy. Thus, lowering the probe temperature to 0 °C caused the broad Cp resonance at δ 5.70 to decoalesce into two sharp, equal-intensity singlets at δ 5.70 and 5.58. The observation of resonances for nonequivalent Cp ligands at this temperature is consistent with η^3 coordination of the allyl fragment to the Cp_2Zr^+ moiety in **2a**. The ^{1}H−^{1}H COSY experiment indicated that the resonances at δ 2.54 and 3.36 are mutually coupled, and the HSQC experiment showed that they are both attached to a carbon atom with a ^{13}C resonance at δ 67.2, supporting in this way their assignment to the CH_2 allyl hydrogens of **2a**. The ^{1}H−^{13}C HMBC spectrum indicated that the two CH_2 allyl resonances at δ 2.54 and 3.36 and the CH_2CHMe_2 resonance at δ 1.94 show cross peaks with a ^{13}C resonance at δ 162, which was ascribed to the central allyl carbon atom of **2a**. In addition, both CH_2 allyl resonances at δ 2.54 and 3.36 exhibit HMBC cross peaks with the ^{13}C resonance at δ 67.2. This is consistent with the presence of two equivalent CH_2 allyl groups which are mutually correlated via

dx.doi.org/10.1021/om400972u | *Organometallics* XXXX, XXX, XXX−XXX

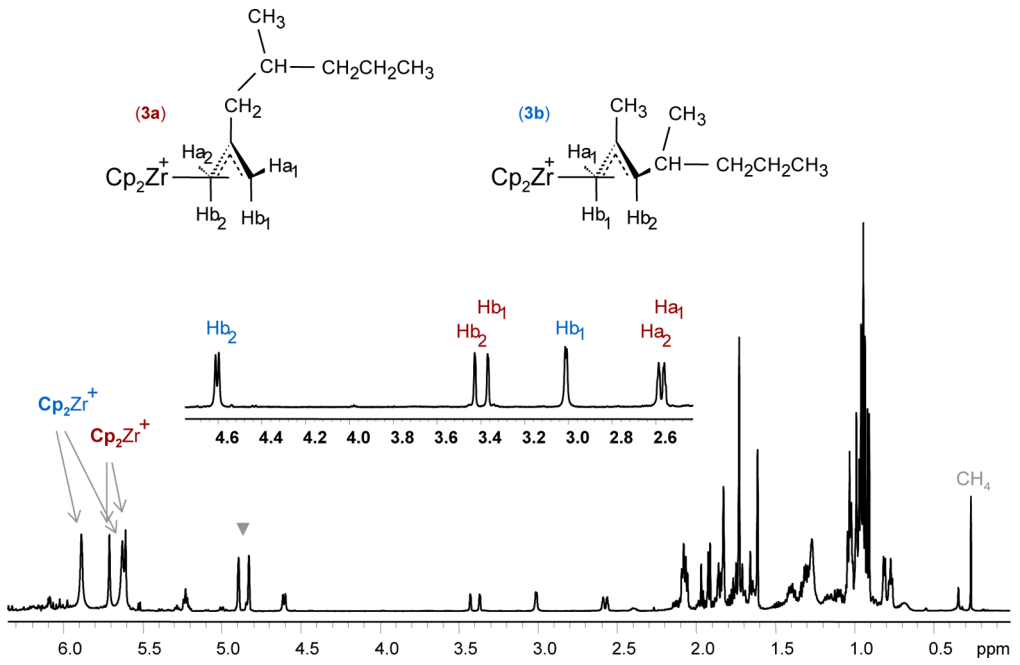

Figure 2. ^{1}H NMR spectrum of the in situ reaction between [Cp_2ZrMe][$MeB(C_6F_5)_3$] and 2,4-dimethyl-1-heptene (1:3 mole ratio) in C_6D_5Cl (600 MHz, 0 °C): (▼) 2,4-dimethyl-1-pentene. The inset shows an expanded scale of the allylic region.

long-range ^{1}H−^{13}C couplings and hence with symmetric bonding of the allyl ligand to zirconium.

A complementary ^{1}H−^{1}H NOESY experiment revealed that the CH_2 allyl resonance at δ 2.54 exhibits strong NOE correlations with the $-CH_2CHMe_2$ (δ 1.94), $-CH_2CHMe_2$ (δ 1.75), and $-CH_2CHMe_2$ (δ 1.01) resonances while the CH_2 allyl resonance at δ 3.36 shows only very weak correlations with the $-CH_2CHMe_2$ (δ 1.94) and $-CH_2CHMe_2$ (δ 1.01) resonances. Also, no NOE correlation between the CH_2 allyl resonance at δ 3.36 and the $-CH_2CHMe_2$ resonance at δ 1.75 was observed. These data indicate that the CH_2 allyl hydrogens which appear at δ 2.54 are syn with respect to the $-CH_2CHMe_2$ group, while those giving rise to the resonance at δ 3.36 are anti. The ^{1}H−^{1}H NOESY spectrum also reveals NOE cross peaks between both Cp resonances and the CH_2 allyl syn and anti hydrogen resonances and between both Cp resonances and the CH_2CHMe_2 resonance, as expected in complex **2a**.

Support for η^3-allyl coordination in **2a** comes also from the one-bond ^{13}C−^{1}H coupling constants of the terminal CH_2 allyl groups. In particular, the magnitude of the $^1J_{CH}$ coupling constants (145 and 159 Hz for the ^{13}C−$^1H_{anti}$ and ^{13}C−$^1H_{syn}$ couplings, respectively) indicates a high degree of unsaturation of the two CH_2 allyl groups,[23] as expected for a η^3-allyl moiety. A larger $^1J_{CH}$ value for syn hydrogens as compared with anti hydrogens has been noted previously,[24] and it was explained in terms of distortions of the η^3-allyl group with respect to the Cp_2Zr^+ moiety in which syn hydrogens are bent from the allyl carbon plane toward the metal, while the anti hydrogens are bent away from the metal,[24] a feature which was also observed by X-ray analysis of similar complexes.[25] Table 1 summarizes the NMR data assigned to the η^3-allyl fragment of **2a**. These data are in good agreement with literature precedents.[17b,18a,c,24]

Small quantities (less than 10% as determined by ^{1}H NMR spectroscopy) of the cationic Zr−allyl complex **2b** were also formed during the reaction. However, due to rapid exchange processes prone to extensive line broadening and averaging of the ^{1}H NMR signals (vide infra), the proton resonances of **2b** could not be easily identified in the ^{1}H NMR spectra of the reaction products acquired at ambient temperature and 0 °C, respectively. These become more evident in the ^{1}H NMR spectra after the probe temperature was lowered to −40 °C. A typical ^{1}H NMR spectrum of the reaction mixture at −40 °C is presented in Figure 1. As can be seen, there is a second set of low, equal-intensity resonances at δ 5.72 (s) and 5.54 (s), ascribed to nonequivalent Cp ligands of **2b**. Weak resonances of comparable intensity are also present at δ 3.75 (d, J_{HH} = 9.4 Hz), 3.29 (d, J_{HH} = 1.9 Hz), and 2.32 (d, J_{HH} = 1.9 Hz). The relative intensity of the resonances at δ 5.72 and 5.54 as compared to the resonances at δ 3.75, 3.29, and 2.32 is 5:1, and on this basis as well as on the basis of proton−proton coupling constants,[23] these resonances were attributed to the allylic CH (δ 3.75) and terminal allylic CH_2 (δ 3.29, 2.32) hydrogens of **2b**. Although the other resonances of **2b** could not be clearly identified at this temperature, the ^{1}H NMR spectrum also shows the presence of a weak resonance at δ 0.44 (d, J_{HH} = 6.0 Hz, 3H), which was attributed to one of the terminal methyl hydrogens of the $CHMe_2$ fragment of **2b**; the other methyl resonance is partially overlapped with the terminal methyl resonance of 2,4-dimethyl-1-pentene at δ 0.94.

Attempts to obtain helpful 2D NMR spectra of complex **2b** at −40 °C were unsuccessful. However, the HSQC and ^{1}H−^{13}C HMBC NMR spectra acquired at 0 °C afforded the observation of ^{13}C NMR resonances for the allyl fragment of **2b** at δ 70 (CH_2 allyl), 159 (central allyl carbon), and 92 (CH allyl, $^1J_{CH}$ = 143 Hz). These ^{13}C NMR data support η^3 coordination of the allyl fragment to zirconium in **2b** and are consistent with literature data for unsymmetrical η^3-allyl complexes.[18c,26] A summary of the NMR data assigned to the η^3-allyl fragment of **2b** is shown in Table 1.

Reaction of [Cp_2ZrMe][$MeB(C_6F_5)_3$] with 2,4-Dimethyl-1-heptene. The reaction of **1** with 2,4-dimethyl-1-heptene was similarly investigated by NMR spectroscopy. As in previous example, treatment of a C_6D_5Cl solution of **1** with 2,4-

dx.doi.org/10.1021/om400972u | Organometallics XXXX, XXX, XXX−XXX

dimethyl-1-heptene at ambient temperature resulted in a slow change in color of the reaction mixture from yellow to orange-brown. The reaction comprising equimolar amounts of 2,4-dimethyl-1-heptene and **1** was complete within 8 h, while the reaction involving a 5-fold excess of 2,4-dimethyl-1-heptene was essentially complete within 1 h.

The progress of the reaction was monitored by ^{1}H NMR spectroscopy, which revealed the gradual disappearance of the *Cp* (δ 5.97) and Zr−*Me* (δ 0.56) resonances of **1** and the 2,4-dimethyl-1-heptene[27] resonances; the *Me*−B (δ 0.34) resonance of **1** broadened and shifted downfield. Concurrently, there appeared a singlet at δ 0.25, attributable to methane. In addition, two different sets of exchange-broadened resonances appeared in the Cp (δ 5.5−6.0) and allylic (δ 2.5−4.7) regions of the ^{1}H NMR spectrum, indicating formation of both cationic Zr−allyl complexes $[Cp_2Zr(\eta^3\text{-}CH_2C(CH_2R)CH_2)]^+$ (**3a**) and $[Cp_2Zr(\eta^3\text{-}CH_2C(Me)CHR)]^+$ (**3b**) (R = CH(Me)-$CH_2CH_2CH_3$) (Scheme 1). Small amounts of unidentified compounds also formed, as indicated by the presence of very weak intensity resonances at δ 5.95−6.30 and 4.95−5.55. Monitoring by ^{1}H NMR spectroscopy revealed that at the beginning of the reaction complex **3a** forms more quickly than complex **3b**. However, as the reaction proceeds, the ratio between complexes **3a** and **3b** becomes almost equal and remains constant until the end of the reaction. When equimolar amounts of **1** and 2,4-dimethyl-1-heptene were used, the two cationic species **3a**,**b** formed in an approximately 1.2:1 ratio; yet, when a high excess (10 equiv) of 2,4-dimethyl-1-heptene was used, the reaction resulted in formation of complex **3a** only. The reason for this behavior is not clear.

The identity of the cationic Zr−allyl complexes **3a**,**b** was again established using a combination of ^{1}H NMR and correlation spectroscopy at low temperature. As expected, the NMR data of complex **3a** at 0 °C are similar to those of complex **2a**. Thus, two separate resonances are observed for the two nonequivalent Cp ligands at δ 5.71 and 5.61. In comparison to **2a**, the allyl ligand of **3a** contains a chiral center and as a result the two terminal CH_2 allyl groups are slightly nonequivalent,[23,28] giving rise to two separate pairs of resonances, one pair at δ 3.42 and 2.58 (^{13}C resonance at δ 68) and the other at δ 3.36 and 2.56 (^{13}C resonance at δ 67) (Figure 2 and Table 1). The ^{13}C NMR resonance of the central allyl carbon atom of **3a** occurs at δ 162. As for **2a**, the allylic CH_2 syn hydrogens were found to resonate at higher magnetic field than the allylic CH_2 anti hydrogens.

The ^{1}H NMR chemical shifts assigned above were also corroborated by a ^{1}H−^{1}H NOESY experiment, which revealed NOE correlations between both Cp resonances at δ 5.71 and 5.61 and the syn (δ 2.58 and 2.56) and anti (δ 3.42 and 3.36) hydrogens of the two CH_2 allyl groups, as expected in **3a**. Furthermore, the $^1J_{CH}$ coupling constants observed for the syn (159 Hz) and anti (145 Hz) hydrogens of the allylic CH_2 groups of **3a** are identical with those observed for **2a**, which suggests that the η^3-allyl ligands in these two complexes adopt a similar spatial arrangement with respect to the Cp_2Zr^+ moiety.

In the case of **3b**, the ^{1}H NMR spectrum at 0 °C (Figure 2) exhibits two resonances for the nonequivalent Cp ligands at δ 5.62 and 5.88, two resonances for the terminal CH_2 allyl hydrogens at δ 3.0 (d, $^2J_{HH}$ = 4.5 Hz) and 1.85 (overlapped) (^{13}C resonance at δ 57), and one resonance for the substituted methyne allyl proton at δ 4.6 (d, $^3J_{HH}$ = 9.1 Hz) (^{13}C resonance at δ 106). On the basis of a ^{1}H−^{1}H NOESY experiment, the CH_2 allyl hydrogen at δ 3.0 and the substituted CH allyl hydrogen at δ 4.6 were found to have an anti arrangement relative to the $-CH_2C(Me)CHCH(Me)Pr$ (Pr = propyl) group, while the CH_2 allyl hydrogen which appears at δ 1.85 was found to have a syn configuration. The ^{13}C resonance of the central allyl carbon atom $CH_2C(Me)CHCH(Me)Pr$ appears at δ 158. Again, these assignments were reinforced by the observation of NOESY correlations between the two Cp resonances at δ 5.62 and 5.88 and the substituted methyne allyl resonance at δ 4.6 and the terminal CH_2 allyl resonances at δ 3.0 and 1.85 and support the η^3 coordination of the allyl unit to the Cp_2Zr^+ moiety in **3b**.

It is noteworthy that the chemical shift of the CH_2 allyl carbon (δ 57) of **3b** is closer to an alkyl carbon chemical shift rather than an olefinic shift (δ 110−150);[23] similarly, the proton−proton coupling constant of the CH_2 allyl hydrogen at δ 3.0 ($^2J_{HH}$ = 4.5 Hz) is much larger than a typical proton−proton coupling constant between two geminal hydrogens on a $=CH_2$ group ($^2J_{HH}$ = 0−2 Hz).[23] The chemical shifts of the substituted CH allyl group (^{13}C resonance, δ 106; ^{1}H resonance, δ 4.6), on the other hand, are closer to olefinic chemical shifts.[23] This implies a high degree of distortion of the allyl ligand of **3b** from an η^3 toward an η^1 configuration, a characteristic which was actually observed in X-ray studies of similar complexes.[29]

Furthermore, for the terminal allylic CH_2 group of **3b**, the $^1J_{CH}$ value for the ^{13}C−$^1H_{syn}$ coupling (157 Hz) is larger than the $^1J_{CH}$ value for the ^{13}C−$^1H_{anti}$ coupling (149 Hz), but both values are typical of an allyl group. The $^1J_{CH}$ value for the substituted methyne allyl group, on the other hand (137 Hz), is out of the range for a $^1J_{CH}$ value of an olefinic group (~140−160 Hz),[23] although both carbon (δ 106) and hydrogen (δ 4.6) resonances of the allylic methyne group are closer to those for the olefinic region. This unusual $^1J_{CH}$ value might be explained by further distortion of the allyl ligand relative to the Cp_2Zr^+ moiety, in which the anti hydrogen of the substituted methyne allyl group is tilted away from the metal while the electron density is accumulating on the metal side of the allyl.[24b]

Dynamic Behavior of $Cp_2Zr^+(\eta^3$-allyl) Species. Earlier reports on several zirconocene η^3-allyl complexes have shown that the allyl ligands of these complexes, in solution, are fluxional.[17a,18] Two main mechanisms have been put forward to explain the fluxional behavior of the metal(η^3-allyl) complexes.[30] The first involves a η^1-coordinated allyl intermediate and consists of an η^3- to η^1-allyl rearrangement by dissociation of one of the allyl carbon−carbon π bonds, rotation of the C=C unit about the allyl carbon−carbon σ-bond and possibly of the η^1-allyl unit about the metal−carbon σ-bond, and reversion to the η^3-allyl coordination mode by recoordination of the allyl carbon−carbon π bond to the metal center (eq 3).[30,31] This mechanism offers a pathway for exchange of the allylic syn and anti hydrogens.

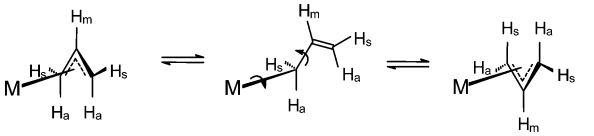

(3)

The second mechanism consists of a 180° rotation of the η^3-coordinated allyl ligand about the metal−allyl bond, as shown in eq 4.[30]

For a particular metal−allyl complex, the fluxional behavior of the allyl ligand can involve any one of these processes, other

dx.doi.org/10.1021/om400972u | *Organometallics* XXXX, XXX, XXX−XXX

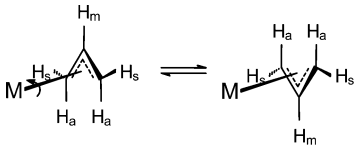

(4)

processes, or a combination of them, which makes the mechanistic interpretation of experimental results rather difficult.[30a]

Variable-temperature ^{1}H NMR spectra of the cationic zirconium-allyl complexes **2a**,**b** and **3a**,**b** described above revealed that the Cp and the allylic proton resonances of these complexes change in shape and shift, reversibly, upon changing the probe temperature. In this section, the dynamic processes responsible for these changes are investigated.

*(a). Dynamic Behavior of the Cationic Complexes [$Cp_2Zr(\eta^3$-$CH_2C(CH_2CHMe_2)CH_2)]^+$ (**2a**) and [$Cp_2Zr(\eta^3$-CH_2C-$(Me)CHCHMe_2)]^+$ (**2b**).* The ^{1}H NMR spectrum of complex **2a** at −40 °C exhibits two singlets for the two nonequivalent Cp ligands at δ 5.61 and 5.52, one singlet for the CH_2 allyl syn hydrogens at δ 2.5, and one singlet for the CH_2 allyl anti hydrogens at δ 3.24, consistent with a virtually static structure of the η^3-allyl ligand of **2a** at this temperature. Upon warming, the Cp resonances decrease in intensity and broaden to coalesce at 20 °C. When the probe temperature is raised further, the broad, averaged Cp resonance becomes narrow and shifts slightly downfield ($\Delta\delta$ = 0.14 between 20 and 70 °C). The allylic CH_2 syn and anti hydrogen resonances, on the other hand, rather diverge than coalesce when the probe temperature is increased from −40 to 60 °C (see Figure 3); moreover, they begin to broaden at about 20 °C and, although they broaden considerably up to 50 °C, they do not coalesce until 70 °C, a temperature for which decomposition also begins to occur. These observations indicate that the Cp ligands of **2a** as well as the allylic syn and anti CH_2 hydrogens of **2a** are exchanging. Both the syn and anti hydrogen exchange and the Cp ligand exchange, respectively, were also observed in a ^{1}H−^{1}H NOESY spectrum recorded at 0 °C. The free energy of activation, as estimated from the coalescence temperature of the Cp ligands, is 59.9 kJ/mol. This is comparable to the free energy of activation found for the 2-methylallyl analogue in C_6D_5Br.[18a]

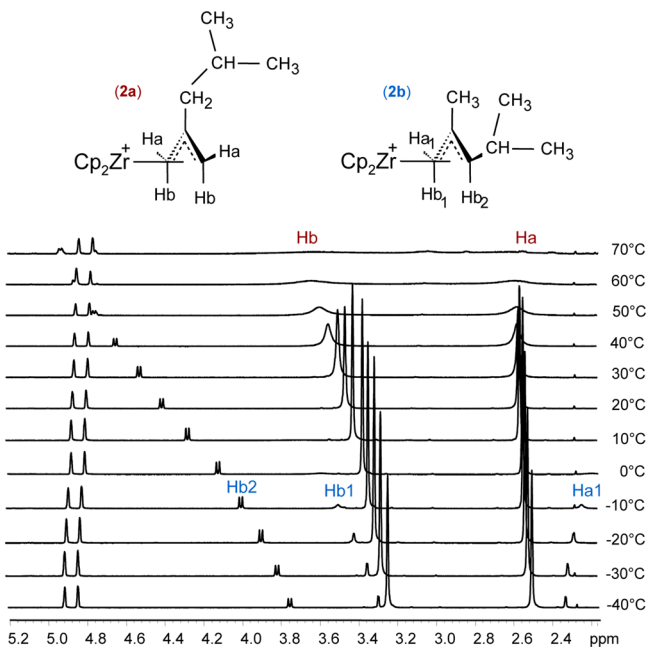

Figure 3. Variation of syn and anti hydrogen resonances of complexes **2a** (red labels) and **2b** (blue labels) with temperature. The peaks marked with Ha and Ha_1 represent syn hydrogen resonances, and the peaks marked with Hb, Hb_1, and Hb_2 represent anti hydrogen resonances.

The intramolecular syn and anti hydrogen exchange in **2a** can be interpreted in terms of η^3- to η^1-allyl rearrangement, rotation of the C═C unit about the allyl carbon−carbon σ bond, and reversion to the η^3-allyl coordination mode, as shown in Scheme 2a. On reversion from the η^1- to η^3-allyl coordination mode, the CH_2CHMe_2 fragment of **2a** can become closer to any one of the two Cp ligands, leading to apparent Cp ligand exchange, as well (see Scheme 2a). Thus, this exchange mechanism would result in equilibration of both the Cp and the CH_2 allyl syn and anti hydrogen resonances, respectively. Nevertheless, the Cp resonances coalescing at a much lower temperature than the allylic CH_2 syn and anti hydrogen resonances was expected, considering the larger chemical shift separation observed in the latter case.[23b] Processes involving rotation of the η^3-allyl group about the Zr−allyl bond may also be contributing to the observed fluxional behavior of **2a**. This exchange mechanism does not involve a η^1-allyl intermediate and thus would result in apparent Cp ligand exchange only, as shown in Scheme 2b.

The ^{1}H NMR spectrum of complex **2b** at −40 °C shows two sharp resonances for the Cp ligands at δ 5.72 and 5.54, one doublet for the allylic CH hydrogen at δ 3.75, and two doublets for the syn and anti hydrogens of the CH_2 allyl group at δ 2.32 and 3.29, respectively. This spectrum is consistent with a virtually static structure of **2b**. When the probe temperature is raised, coalescence of the Cp signals occurs at 0 °C, which translates into a free energy of activation for the Cp ligand exchange of 54.1 kJ/mol. Upon further warming, the averaged Cp resonance narrows and shifts downfield ($\Delta\delta$ 0.36 between 0 and 70 °C). As with **2a**, when the probe temperature is raised the syn and anti CH_2 allyl hydrogen resonances diverge and broaden considerably such that, at 0 °C, they have completely disappeared into the baseline (Figure 3). These results imply that the allyl ligand of **2b** also undergoes a dynamic process in which both the CH_2 allyl syn and anti hydrogens and the Cp ligands are exchanging, respectively. A mechanism which would account for the syn and anti hydrogen exchange at the CH_2 allyl terminus consists of dissociation of the carbon−carbon π bond at the monosubstituted CH allyl end, rotation about the allyl carbon−carbon σ bond, and recoordination of the carbon−carbon π bond to zirconium. This mechanism would also result in the apparent Cp ligand exchange.

Of special interest in this case, however, is the observation that, when the probe temperature is raised, the allylic C*H* resonance of **2b** is significantly shifted downfield from δ 3.75 at −40 °C toward a free alkene position (δ 4.93) at 70 °C. Concurrently, the *Me*−B resonance of the free $[MeB(C_6F_5)_3]^-$ anion broadens and shifts upfield from δ 1.38 at −40 °C to about δ 1.0 at 50 °C. In addition, when the probe temperature reaches 40 °C, a very weak, broad resonance, presumably the *Me*−B resonance of the $[MeB(C_6F_5)_3]^-$ anion coordinating to **2b**, emerges at δ 0.44; this new resonance narrows somewhat and shifts slightly upfield to δ 0.37 upon further warming to 70 °C. When the probe temperature is lowered, the same chemical shift changes occur in reverse.

dx.doi.org/10.1021/om400972u | *Organometallics* XXXX, XXX, XXX−XXX

Scheme 2. Proposed Mechanism for (a) Syn−Anti Hydrogen Exchange and Apparent Cp Ligand Exchange and (b) Apparent Cp Ligand Exchange in Complex 2a

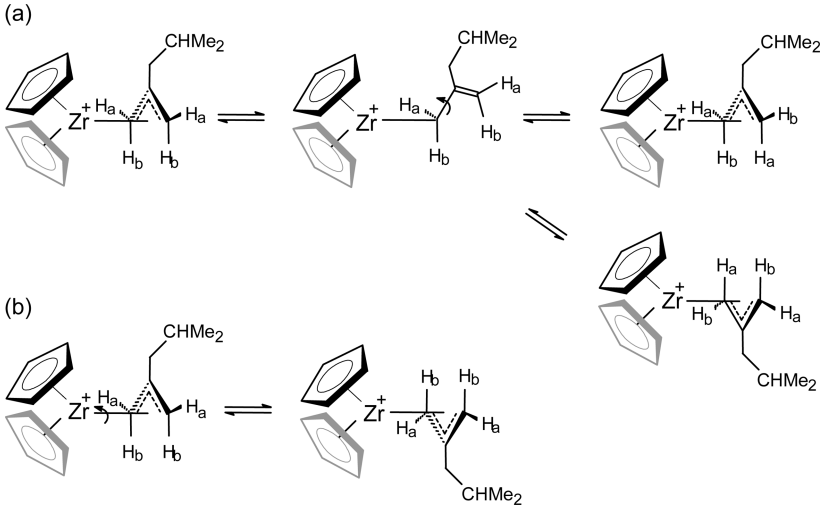

The substantial shift of the allylic C*H* resonance with temperature together with the changes of the averaged Cp and the *Me*−B chemical shifts with temperature can be best explained in terms of a rapid equilibrium between two species, the η^3-coordinated allyl complex **2b** and the η^1 complex $[Cp_2Zr(\eta^1\text{-}CH_2C(Me)=CHCHMe_2]^+$, and between the free and coordinated $[MeB(C_6F_5)_3]^-$ anion, as shown in Scheme 3.

Scheme 3. Equilibrium between the η^1- and η^3-Coordinated Allyl Complexes of 2b

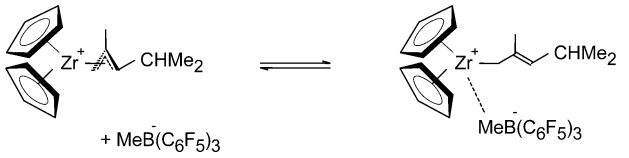

The existence of a rapid equilibrium between the η^3- and η^1-coordinated allyl complexes of **2b** might also explain the divergence of the syn and anti CH_2 allyl hydrogens of **2b** with increasing temperature. Thus, the chemical shift position of the averaged CH allyl resonance observed depends on the composition of the equilibrium mixture at various temperatures,[23b] namely

$$\delta_{obs} = p_1\delta_1 + p_2\delta_2 \quad (5)$$

where p_1 and δ_1 are the mole fraction and chemical shift, respectively, of the η^3-coordinated allyl complex and p_2 and δ_2 are the mole fraction and chemical shift of the η^1-coordinated allyl complex, respectively ($p_1 + p_2 = 1$). Considering that the proton resonance at δ 3.75, recorded at −40 °C, corresponds mostly to the monosubstituted CH allyl hydrogen of the η^3-coordinated allyl ligand of **2b** and that the proton resonance at δ 4.93, recorded at 70 °C, corresponds mostly to the =CH hydrogen of the η^1-coordinated allyl ligand of **2b**, temperature-dependent mole fractions of η^3- and η^1-coordinated allyl complexes can thus be estimated. For instance, at 20 °C, roughly 55% of the **2b** complexes are predicted to have η^1 coordination.

Similar temperature-dependent changes of the averaged Cp and allylic CH_2 hydrogen chemical shifts were also observed for **2a** (vide supra). By analogy with **2b**, these changes can also be interpreted in terms of a rapid equilibrium between the η^3- and η^1-coordinated allyl complexes of **2a**. From a comparison between the chemical shift changes of the averaged Cp resonances of complexes **2a**,**b** ($\Delta\delta$ 0.14 vs $\Delta\delta$ 0.36, respectively), it can be inferred that at high temperatures the mole fraction of η^1-coordinated allyl complex present at equilibrium is much lower for **2a** than for **2b**. A lower fraction of the η^1-allyl complex present at equilibrium in the case of **2a** is also consistent with the higher free energy of activation found in this case, as the η^1-allyl species is a key intermediate in the exchange processes involving the rotation of the C=C unit about the allyl carbon−carbon σ bond.

*(b). Dynamic Behavior of the Cationic Complexes $[Cp_2Zr(\eta^3\text{-}CH_2C(CH_2CH(Me)(Pr))CH_2)]^+$ (**3a**) and $[Cp_2Zr(\eta^3\text{-}CH_2C(Me)(CHCH(Me)(Pr))]^+$ (**3b**).* The variable-temperature ^{1}H NMR spectra acquired for complex **3a** are to a great extent similar to those obtained for complex **2a**. Thus, at −40 °C, the ^{1}H NMR spectrum of **3a** exhibits two sharp resonances for the two nonequivalent Cp ligands at δ 5.62 and 5.54, two singlets for the two CH_2 allyl syn hydrogens at δ 2.55 and 2.53, and two singlets for the two CH_2 allyl anti hydrogens at δ 3.31 and 3.24. When the temperature is raised, the Cp resonances broaden and coalesce to 20 °C. The free energy of activation for this process is 60.2 kJ/mol, similar to that estimated for **2a**. The CH_2 allyl syn and anti hydrogen resonances are broadened and divergently shifted at this temperature (Figure 4). As for **2a**, upon further warming, the averaged Cp resonance narrows and shifts slightly downfield while the CH_2 allyl syn and anti hydrogen resonances broaden considerably but do not coalesce up to 60 °C. Again, these data indicate that the Cp ligands and the CH_2 allyl syn and anti hydrogens of **3a** are exchanging, respectively, and that, similar to the case for **2a**, the η^3-coordinated allyl complex of **3a** exists in solution in a rapid equilibrium with the η^1-coordinated allyl complex of **3a**.

A mechanism which would account for the syn/anti hydrogen exchange in **3a** consists of dissociation of the carbon−carbon π bond at one CH_2 allyl terminus, rotation of the C=C unit about the allyl carbon−carbon σ bond as well as the zirconium−carbon σ bond, and recoordination of the carbon−carbon π bond to zirconium, as shown in Scheme 4. Depending on the direction of rotation of the η^1-coordinated allyl unit about the zirconium−carbon σ bond, there is a

dx.doi.org/10.1021/om400972u | *Organometallics* XXXX, XXX, XXX−XXX

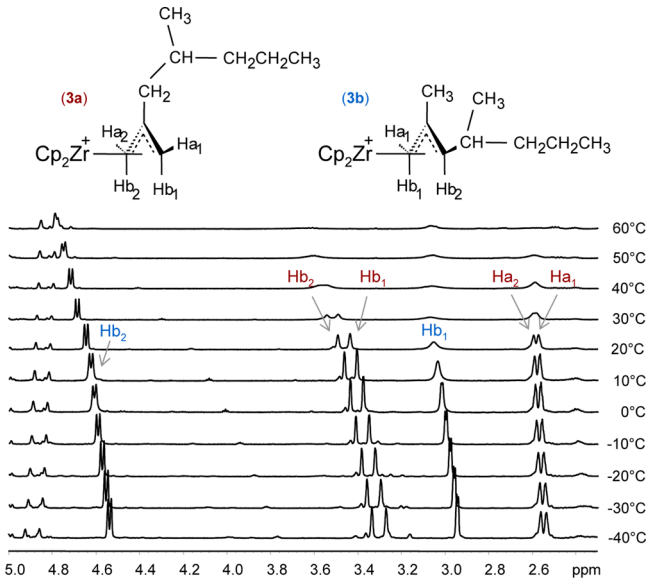

Figure 4. Variable-temperature ^{1}H NMR spectra of a mixture of complexes **3a** (red labels) and **3b** (blue labels) in the allyl region in C_6D_5Cl at 600 MHz (counterion, $[MeB(C_6F_5)_3]^-$). The peaks marked with Ha_1 and Ha_2 represent syn hydrogen resonances, and the peaks marked with Hb_1 and Hb_2 represent anti hydrogen resonances.

roughly equal probability that the apparent Cp ligand exchange also takes place (compare Scheme 4a with Scheme 4b). This exchange mechanism is also supported by a ^{1}H−^{1}H NOESY experiment run at 0 °C. In particular, the ^{1}H−^{1}H NOESY spectrum of **3a** at 0 °C (Figure 5) shows definite exchange cross peaks between the syn hydrogen of the C_1 (Ha_1) and the anti hydrogen of the C_2 (Hb_2), as well as between the syn hydrogen of C_2 (Ha_2) and the anti hydrogen of C_1 (Hb_1). Apart from the syn/anti hydrogen exchange, the exchange mechanism displayed in Scheme 4 also results in syn/syn and anti/anti hydrogen exchange. However, this exchange cannot be observed in the ^{1}H−^{1}H NOESY spectrum, most probably due to the poor resolution of the spectrum. As for **2a**, a mechanism involving the rotation of the η^3-coordinated allyl ligand about the metal−allyl bond, which would result in apparent Cp ligand exchange, cannot be ruled out for **3a**.

It is worth noting that, in addition to the intramolecular syn and anti hydrogen exchange, rotation of the C═C unit about the allyl carbon−carbon σ bond (Scheme 4) also results in a change of the allyl coordination face relative to zirconium and, as a result, the two ends of the allyl group also exchange. The reversal of the η^3-allyl coordination face relative to zirconium might actually be a common feature in the complexes which undergo syn/anti hydrogen exchange. Nevertheless, this type of exchange cannot be observed in the metal(η^3-allyl) complexes in which the two ends of the allyl group are equivalent.

In the case of **3b**, the ^{1}H NMR spectrum at −40 °C shows two singlets for the two Cp ligands at δ 5.83 and 5.56, one doublet for the allyl CH hydrogen at δ 4.52, and two doublets

Scheme 4. Proposed Mechanism of Syn−Anti Hydrogen Exchange and Apparent Cp Ligand Exchange in Complex 3a: (a) Syn/Anti, Syn/Syn, and Anti/Anti Hydrogen Exchange ($Ha_2 \rightarrow Ha_1$, $Ha_1 \rightarrow Hb_2$, $Hb_2 \rightarrow Hb_1$, $Hb_1 \rightarrow Ha_2$); (b) Syn/Anti, Syn/Syn, and Anti/Anti Hydrogen Exchange as Well as Apparent Cp Ligand Exchange

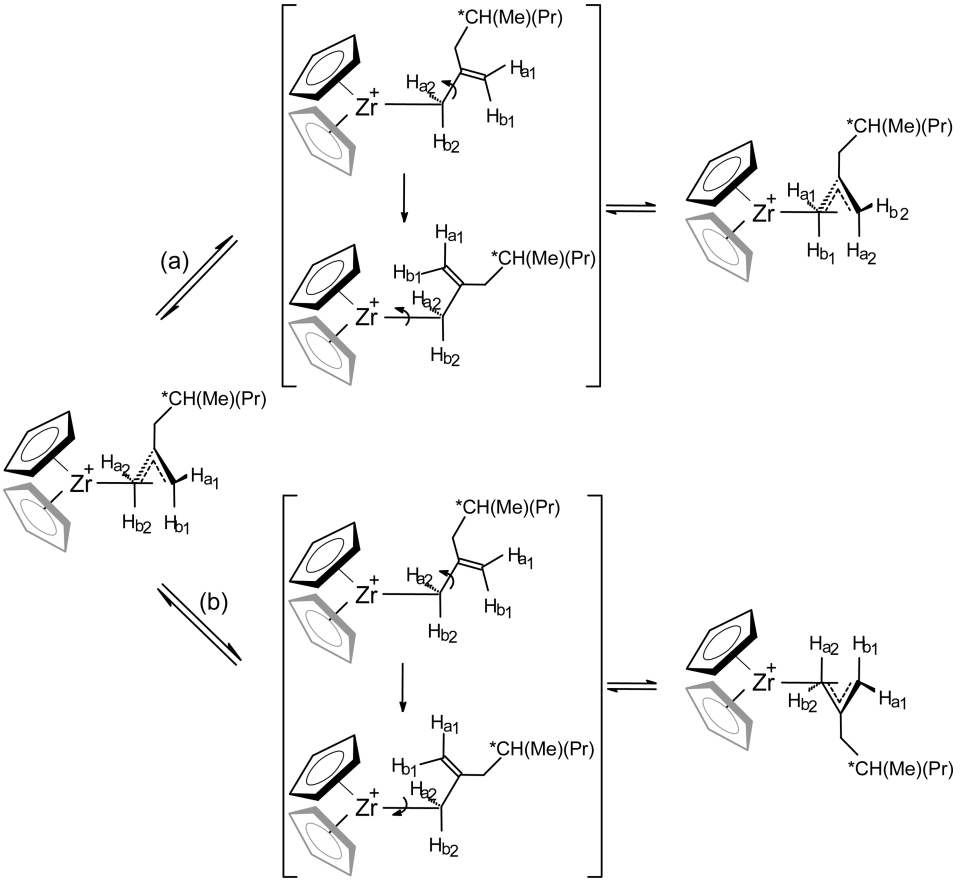

dx.doi.org/10.1021/om400972u | Organometallics XXXX, XXX, XXX−XXX

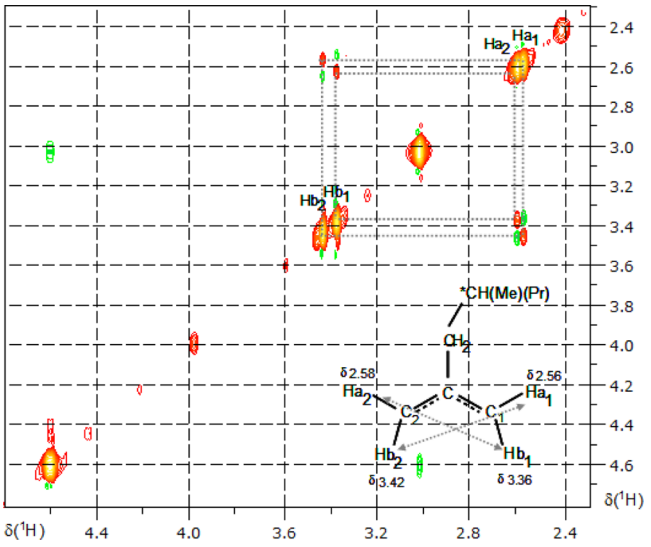

Figure 5. ^{1}H−^{1}H NOESY spectrum of complex **3a** in the allylic region (0 °C, 600 MHz, mixing time 0.4 s). The exchange cross peaks are in red, while the NOE cross peaks are in green. Inset: chemical structure of the allyl ligand of **3a**, with chemical shift assignments (δ in ppm). Ha_1 and Hb_1 are syn and anti hydrogens, respectively, on carbon C_1, and Ha_2 and Hb_2 are the syn and anti hydrogens on carbon C_2.

for the two CH_2 allyl syn and anti hydrogens at δ 1.83 and 2.93, respectively. When the temperature is raised, the Cp resonances and the allylic syn and anti hydrogen resonances begin to broaden, and while the Cp resonances coalesce at approximately 30 °C, coalescence for the syn and anti hydrogens of the allylic CH_2 group does not occur up to 60 °C (Figure 4). The averaged Cp resonance, on the other hand, narrows and shifts slightly downfield as the temperature is increased from 30 to 60 °C. The intramolecular syn and anti hydrogen exchange observed in this case is expected to proceed via a mechanism similar to that described for **2b** (vide supra). The experimental free energy of activation estimated from the coalescence of the Cp resonances of **3b** is 60.2 kJ/mol, about 6 kJ/mol higher than that estimated for **2b**. A higher free energy of activation in this case can be related to the greater steric interactions in **3b**.[23b]

It is notable that the chemical shift of the allylic CH hydrogen of **3b** at −40 °C is very close to an olefinic chemical shift and it only shifts slightly downfield ($\Delta\delta$ = 0.26) when the probe temperature is raised from −40 to 60 °C. As with **2b**, the dependence of the allylic C*H* chemical shift on temperature implies the existence of a rapid equilibrium between the η^3- and η^1-coordinated allyl complexes of **3b**. However, a greatly deshielded chemical shift of the CH allyl hydrogen of **3b** at −40 °C (δ 4.52 for complex **3b** as compared with δ 3.75 for complex **2b**) coupled with the smaller variation in the chemical shift position observed when the temperature is increased to 60 °C ($\Delta\delta$ = 0.26 for complex **3b** as compared with $\Delta\delta$ = 1.18 for complex **2b**) might indicate that, while complex **2b** is found predominantly as a η^3-allyl complex at −40 °C, complex **3b** is found mostly as a η^1-allyl complex.

SUMMARY

Reactions between Cp_2ZrMe_2 activated with $B(C_6F_5)_3$ and 2,4-dimethyl-1-pentene and 2,4-dimethyl-1-heptene, respectively, in C_6D_5Cl at ambient temperature, result in the irreversible formation of Zr−allyl complexes **2a**,**b** and **3a**,**b** along with methane. These complexes have been characterized in solution by one- and two-dimensional NMR spectroscopy with regard to their structure and dynamic behavior.

Variable-temperature one- and two-dimensional NMR experiments indicated that the allyl ligands of complexes **2a**,**b** and **3a**,**b** are fluxional. The dynamic behavior of these complexes is mainly due to the η^3 to η^1 isomerization, rotation of the carbon−carbon π unit about the allyl carbon−carbon σ bond, and reversion to the η^3-allyl coordination mode, when the CH_2 allyl syn and anti hydrogen exchange as well as the apparent Cp ligand exchange occurs. The rotation of the C═C unit about the allyl carbon−carbon σ bond also results in a change of the allyl coordination face relative to the Cp_2Zr^+ moiety, and as a result, the two CH_2 allyl end groups also exchange. A second mechanism which may account for the apparent Cp ligand exchange in the Cp_2Zr^+−allyl complexes under investigation and which consists of rotation of the η^3-coordinated allyl ligand about the metal−allyl bond can also occur. The free energy of activation for the exchange processes, as estimated from the coalescence temperature of the two Cp ligands, is between 54 and 60 kJ/mol. Aside from the intramolecular exchange processes described above, this study also shows that the η^1- and η^3-coordinated allyl species of a particular Zr−allyl complex coexist in solution and that the equilibrium composition of these species is temperature dependent. The Cp_2Zr^+−allyl complexes synthesized and characterized in this paper can serve as excellent models for similar Zr−allyl intermediates which might form during coordination (Ziegler−Natta) polymerization of alkene.

EXPERIMENTAL SECTION

General Considerations. Handling and storage of air-/moisture-sensitive organometallic compounds was done using an MBraun Labmaster glovebox. Chlorobenzene-d_5 was purchased from Cambridge Isotope Laboratories (>99 atom % D) and dried by vacuum distillation from CaH_2, stored over molecular sieves, and handled in the glovebox. Cp_2ZrMe_2 and $B(C_6F_5)_3$ were synthesized as described below. 2,4-Dimethyl-1-pentene and 2,4-dimethyl-1-heptene were obtained from ChemSampCo. All other chemicals were purchased from Aldrich.

1D and 2D NMR experiments were performed on a Bruker AV 600 spectrometer, chemical shifts being referenced using the residual proton signals of chlorobenzene-d_5. Probe temperatures were calibrated using methanol (low temperature) and ethylene glycol (high temperature) samples as references. ^{1}H NMR spectra were acquired with a 45° pulse and 1 s delay between pulses; 16 transients were stored for each spectrum. ^{1}H−^{13}C HMBC spectra were obtained via heteronuclear zero and double quantum coherence optimized on long-range couplings of 5 Hz, with a low-pass J filter to suppress one-bond correlations and no decoupling during acquisition using gradient pulses for selection. The HMBC acquisition parameters were as follows: a 0.1705 s acquisition time, a 10 ppm spectral window in f2, a 222.3 ppm spectral window in f1, and a 1 s relaxation delay. ^{1}H−^{13}C HSQC spectra were collected using Echo/Antiecho-TPPI gradient selection with decoupling (or with no decoupling, respectively) during acquisition using shaped pulses for all 180° pulses on the f2 channel. The HSQC acquisition parameters were as follows: a 0.1705 s acquisition time, a 10 ppm spectral window in f2, a 165.6 ppm spectral window in f1, and a 1 s relaxation delay. ^{1}H−^{1}H NOESY spectra were recorded using 2D homonuclear correlation via dipolar coupling (due to nuclear Overhauser enhancement (NOE) or chemical exchange); phase sensitive using Echo/Antiecho-TPPI gradient selection, with gradient pulses in mixing time. The NOESY acquisition parameters were as follows: a 0.1672 s acquisition time, a 10.2 spectral window in f2 and f1, respectively, a 2 s relaxation delay, and a 0.4 s mixing time.

Synthesis of Dimethylzirconocene. Dimethylzirconocene was synthesized by a procedure similar to that described in the

dx.doi.org/10.1021/om400972u | *Organometallics* XXXX, XXX, XXX−XXX

literature.[20a,b] Methyllithium (9 mL, 1.4 M in diethyl ether) was added dropwise over a period of 45 min to a stirred suspension of zirconocene dichloride (1.75 g, 6 mmol) in 20 mL of dry diethyl ether under argon at −20 °C, and the reaction mixture was stirred at this temperature for an additional 30 min. After the mixture was warmed to ambient temperature, the solvent was removed under reduced pressure. The residue was extracted with hexane, the extract was filtered, the solvent was evaporated under reduced pressure, and the product was purified by recrystallization from hexane. Alternatively, the product was purified by sublimation at 70 °C. Dimethylzirconocene was obtained as a white powder in a yield of 60.4%.

^{1}H NMR (300 MHz, CD_2Cl_2): δ 6.1 (s, 10H, Cp), −0.41 (s, 6H, Me) ppm. ^{1}H NMR (400 MHz, $C_6D_5CD_3$): δ 5.7 (s, 10H, Cp), −0.21 (s, 6H, Me) ppm.

Synthesis of Tris(pentafluorophenyl)boron. Tris(pentafluorophenyl)boron was synthesized by a modified procedure of Massey and Park.[20c] A solution of butyllithium (33 mL, 53 mmol, 1.6 M solution in hexane) was added dropwise over 3 h under argon to a stirred solution of bromopentafluorobenzene (6 mL, 48.1 mmol) in 300 mL of dry hexane at −78 °C with stirring. The resulting white suspension was stirred at −78 °C for an additional 3 h, at which point boron trichloride (16 mL, 16 mmol, 1 M solution in hexane) was added all at once and the stirring was continued for another 1 h. The reaction mixture was warmed to ambient temperature and filtered to remove LiCl, and then the solvent was removed in vacuo. Tris(pentafluorophenyl)boron was obtained as white crystals in a yield of 25%.

^{19}F NMR (400 MHz, CD_2Cl_2): δ −128 (br s, 6F, *o*-F), −145 (t, 3F, *p*-F), −161 (m, 6F, *m*-F) ppm; lit.[12] ^{19}F NMR (CD_2Cl_2) δ −128 (br s, 6F, *o*-F), −144 (t, 3F, *p*-F), −161 (m, 6F, *m*-F) ppm.

In Situ Reaction between [Cp_2ZrMe][$MeB(C_6F_5)_3$] and 2,4-Dimethyl-1-pentene. A solution of Cp_2ZrMe_2 (40 μmol) in C_6D_5Cl (0.5 mL) was added to a solution of $B(C_6F_5)_3$ (1.1 equiv) in C_6D_5Cl (0.5 mL), and the yellow ion pair solution thus generated was transferred to an NMR tube. The NMR tube was sealed with a rubber septum and Parafilm and removed from the glovebox. Prior to the NMR experiment, 2,4-dimethyl-1-pentene (1−5 equiv) was injected into the NMR tube via a microsyringe at ambient temperature. The progress of the reaction was monitored by ^{1}H NMR spectroscopy. The reaction products could not be isolated and were characterized in solution by ^{1}H NMR and correlation spectroscopy.

In Situ Reaction between [Cp_2ZrMe][$MeB(C_6F_5)_3$] and 2,4-Dimethyl-1-heptene. A solution of Cp_2ZrMe_2 (40 μmol) in C_6D_5Cl (0.5 mL) was added to a solution of $B(C_6F_5)_3$ (1.1 equiv) in C_6D_5Cl (0.5 mL), and the yellow ion pair solution thus generated was transferred to an NMR tube. The NMR tube was sealed with a rubber septum and Parafilm and removed from the glovebox. Prior to the NMR experiment, 2,4-dimethyl-1-heptene (1−10 equiv) was injected in the NMR tube via a microsyringe at ambient temperature. The progress of the reaction was monitored by ^{1}H NMR spectroscopy. The reaction products could not be isolated and were characterized in solution by ^{1}H NMR and correlation spectroscopy.

In Situ Reaction between [Cp_2ZrMe][$MeB(C_6F_5)_3$] and CD_3CN. A solution of Cp_2ZrMe_2 (40 μmol) in C_6D_5Cl (0.5 mL) was added to a solution of $B(C_6F_5)_3$ (1.1 equiv) in C_6D_5Cl (0.5 mL), and the yellow ion pair solution thus formed was charged in an NMR tube. The NMR tube was capped with a septum and removed from the glovebox. The yellow ion pair solution was characterized by ^{1}H NMR spectroscopy. After the ^{1}H NMR spectrum was recorded, 3 equiv of CD_3CN was injected into the NMR tube via a microsyringe at ambient temperature; the NMR tube was shaken vigorously, after which a new ^{1}H NMR spectrum was acquired.

General Procedure for Variable-Temperature ^{1}H NMR Experiments. Samples of Cp_2Zr^+−allyl complexes used for variable-temperature ^{1}H NMR studies were prepared as described above. Samples were brought to the indicated temperature and allowed to equilibrate for 7−10 min before the ^{1}H NMR spectra were acquired. All of the temperature-dependent changes are reversible: i.e., when the probe temperature is lowered, the reverse chemical shift changes occur. The free energies of activation ($\Delta G^{\ddagger}$) were calculated in kJ/mol from the equation $\Delta G^{\ddagger} = RT[23.76\ \ln(k/T)]$, where R is the gas constant (8.3145 J/(mol K)), T is the absolute temperature (K), and k is the rate constant (s^{-1}). The rate constant at the coalescence temperature was approximated using the relation $k_{coal} = \pi\Delta\nu/\sqrt{2} = 2.22\Delta\nu$, where $\Delta\nu$ is the frequency difference (Hz) of decoalesced resonances measured at the temperature of the frozen spectrum. Making the substitution, one obtains $\Delta G^{\ddagger} = RT_c[23.76 - \ln(2.22\Delta\nu/T_c)]$, where T_c is the coalescence temperature (K).[23b]

NMR Spectroscopic Data of [$Cp_2Zr(\eta^3$-$CH_2C(CH_2CHMe_2)$-$CH_2)$]$^+$ (2a). ^{1}H NMR (600 MHz, C_6D_5Cl, 0 °C): δ 5.7 (s, C_5H_5, 5H), 5.58 (s, C_5H_5, 5H), 3.36 (s, allyl H_a, 2H), 2.54 (s, allyl H_s, 2H), 1.94 (d, CH_2, 2H), 1.75 (m, CH, 1H), 1.01 (d, CH_3, 6H) ppm. ^{1}H NMR (600 MHz, C_6D_5Cl, −40 °C): δ 5.61 (s, C_5H_5, 5H), 5.52 (s, C_5H_5, 5H), 3.24 (s, allyl H_a, 2H), 2.5 (s, allyl H_s, 2H), 1.88 (d, $^3J_{HH}$ = 6.8 Hz, CH_2, 2H), 1.74 (m, CH, 1H), 1.02 (d, $^3J_{HH}$ = 6.8 Hz, CH_3, 6H) ppm. ^{13}C NMR (600 MHz, C_6D_5Cl, 0 °C): δ 111.7 (C_5H_5, $^1J_{C-H}$ = 175 Hz), δ 110.5 (C_5H_5, $^1J_{C-H}$ = 175 Hz), 67.2 (allyl CH_2, $^1J_{C-Hanti}$ = 145 Hz, $^1J_{C-Hsyn}$ = 159 Hz), 52 (CH_2, $^1J_{C-H}$ = 131 Hz), 31.1 (CH, $^1J_{C-H}$ = 126 Hz), 22.1 (CH_3, $^1J_{C-H}$ = 129 Hz) ppm.

NMR Spectroscopic Data of [$Cp_2Zr(\eta^3$-$CH_2C(Me)$-$(CHCHMe_2)$)]$^+$ (2b). ^{1}H NMR (600 MHz, C_6D_5Cl, −40 °C): δ 5.72 (s, C_5H_5, 5H), 5.54 (s, C_5H_5, 5H), 3.75 (d, $^3J_{HH}$ = 9.4 Hz, allyl CH, 1H), 3.29 (d, $^2J_{HH}$ = 1.9 Hz, allyl H_a, 1H), 2.32 (d, $^2J_{HH}$ = 1.9 Hz, allyl H_s, 1H) ppm. The other resonances are obscured.

NMR Spectroscopic Data of [$Cp_2Zr(\eta^3$-$CH_2C(CH_2CH(Me)$-$C_3H_7)CH_2)$]$^+$ (3a). ^{1}H NMR (600 MHz, C_6D_5Cl, 0 °C, the resonances were assigned by using correlation spectroscopy): δ 5.71 (s, C_5H_5, 5H), 5.61 (s, C_5H_5, 5H), 3.42 (s, allyl CH_2, H_a, 1H), 3.36 (s, allyl CH_2, H_a, 1H), 2.58 (s, allyl CH_2, H_s, 1H), 2.56 (s, allyl CH_2, H_s, 1H), 2.14 (dd, CH_2, 1H), 1.89 (CH_2, 1H), 1.64 (CH, 1H), 0.99 (CH_3, 3H), 1.18 (CH_2, 1H), 1.39 (CH_2, 1H) ppm. The terminal ethyl resonances are obscured by similar peaks of complex **3b** and unreacted 2,4-dimethyl-1-heptene. ^{1}H NMR (600 MHz, C_6D_5Cl, −40 °C): δ 5.62 (d, $^3J_{HH}$ = 1.5 Hz, C_5H_5, 5H), 5.54 (d, $^3J_{HH}$ = 1.5 Hz, C_5H_5, 5H), 3.31 (s, allyl CH_2, H_a, 1H), 3.24 (s, allyl CH_2, H_a, 1H), 2.55 (s, allyl CH_2, H_s, 1H), 2.53 (s, allyl CH_2, H_s, 1H) ppm.

NMR Spectroscopic Data of [$Cp_2Zr(\eta^3$-$CH_2C(Me)(CHCH(Me)$-$C_3H_7)$]$^+$ (3b). ^{1}H NMR (600 MHz, C_6D_5Cl, 0 °C): δ 5.88 (s, C_5H_5, 5H), 5.62 (s, C_5H_5, 5H), 4.60 (d, $^3J_{HH}$ = 9.1 Hz, allyl CH, 1H), 3.01 (s, $^2J_{HH}$ = 4.5 Hz, allyl CH_2, H_a, 1H), 1.85 (s, allyl CH_2, H_s, 1H), 1.82 (s, CH_3, 3H), 1.70 (CH, 1H), 0.81 (d, CH_3, 3H), 1.17 (CH_2, 1H), 0.88 (CH_2, 1H), 0.78 (CH_2, 1H), 0.67 (CH_2, 1H), 0.77 (t, CH_3, 3H) ppm. ^{1}H NMR (600 MHz, C_6D_5Cl, −40 °C): δ 5.83 (d, $^3J_{HH}$ = 1.5 Hz, C_5H_5, 5H), 5.56 (d, $^2J_{HH}$ = 1.5 Hz, C_5H_5, 5H), 4.52 (d, $^3J_{HH}$ = 9.1 Hz, allyl CH, 1H), 2.93 (d, $^2J_{HH}$ = 4.5 Hz, allyl CH_2, H_a, 1H), 1.83 (d, $^2J_{HH}$ = 4.5 Hz, allyl CH_2, H_s, 1H) ppm.

NMR Spectroscopic Data of [Cp_2ZrMe][$MeB(C_6F_5)_3$]. ^{1}H NMR (600 MHz, C_6D_5Cl, 25 °C): δ 5.97 (s, C_5H_5, 10H), 0.56 (s, Zr-CH_3, 3H), 0.34 (br s, B−CH_3, 3H) ppm. ^{1}H NMR (600 MHz, C_6D_5Cl, 0 °C): δ 5.93 (s, C_5H_5, 10H), 0.55 (s, Zr−CH_3, 3H), 0.33 (br s, B−CH_3, 3H) ppm.

NMR Spectroscopic Data of [$Cp_2Zr(Me)(CD_3CN)$][$MeB(C_6F_5)_3$]. ^{1}H NMR (600 MHz, C_6D_5Cl, 25 °C): δ 5.83 (s, C_5H_5, 10H), 0.22 (s, Zr−CH_3, 3H), 1.16 (br s, B−CH_3, 3H) ppm. ^{1}H NMR (600 MHz, C_6D_5Cl, 0 °C): δ 5.80 (s, C_5H_5, 10H), 0.20 (s, Zr−CH_3, 3H), 1.21 (br s, B−CH_3, 3H) ppm.

AUTHOR INFORMATION

Notes

The authors declare no competing financial interest.

ACKNOWLEDGMENTS

Financial support from Queen's University is gratefully acknowledged. I thank Dr. Francoise Sauriol for her assistance with NMR spectroscopy and useful discussions. I also thank Dr. Natalie M. Cann and Dr. Richard F. Jordan for useful discussions and advice.

REFERENCES

(1) For useful reviews see: (a) Möhring, P. C.; Coville, N. J. *J. Organomet. Chem.* **1994**, *479*, 1. (b) Gupta, V. K.; Satish, S.; Bhardwaj, I. S. *J. Macromol. Sci., Rev. Macromol. Chem. Phys.* **1994**, *C34*, 439. (c) Bochmann, M. *J. Chem. Soc., Dalton Trans.* **1996**, 255. (d) Kaminsky, W.; Arndt, M. *Adv. Polym. Sci.* **1997**, *127*, 143. (e) Scheirs, J., Kaminsky, W., Eds. *Metallocene-based Polyolefins*; Wiley: Chichester, U.K., 1999. (f) Coates, G. W. *Chem. Rev.* **2000**, *100*, 1223. (g) Resconi, L.; Cavallo, L.; Fait, A.; Piemontesi, F. *Chem. Rev.* **2000**, *100*, 1253. (h) Rappé, A. K.; Skiff, W. M.; Casewit, C. J. *Chem. Rev.* **2000**, *100*, 1435. (i) Pédeutour, J.-N.; Radhakrishnan, K.; Cramail, H.; Deffieux, A. *Macromol. Rapid Commun.* **2001**, *22*, 1095.

(2) (a) Brintzinger, H.-H.; Fischer, D.; Mülhaupt, R.; Rieger, B.; Waymouth, R. M. *Angew. Chem., Int. Ed. Engl.* **1995**, *34*, 1143. (b) Bochmann, M. *Top. Catal.* **1999**, *7*, 9. (c) Fischer, D.; Mülhaupt, R. *J. Organomet. Chem.* **1991**, *417*, C7. (d) Chien, J. C. W.; Sugimoto, R. *J. Polym. Sci., Part A: Polym. Chem.* **1991**, *29*, 459. (e) Dornik, H. P.; Luft, G.; Rau, A.; Wieczorek, T. *Macromol. Mater. Eng.* **2004**, *289*, 475. (f) Janiak, C.; Lange, K. C. H.; Marquardt, P. *J. Mol. Catal. A: Chem.* **2002**, *180*, 43. (g) Stehling, U.; Diebold, J.; Kirsten, R.; Röll, W.; Brintzinger, H.-H. *Organometallics* **1994**, *13*, 964. (h) Thorshaug, K.; Støvneng, J. A.; Rytter, E.; Ystenes, M. *Macromolecules* **1998**, *31*, 7149.

(3) (a) Wondimagegn, T.; Xu, Z.; Vanka, K.; Ziegler, T. *Organometallics* **2004**, *23*, 3847. (b) Margl, P. M.; Woo, T. K.; Ziegler, T. *Organometallics* **1998**, *17*, 4997.

(4) (a) Moscardi, G.; Piemontesi, F.; Resconi, L. *Organometallics* **1999**, *18*, 5264. (b) Lin, S.; Kravchenko, R.; Waymouth, R. M. *J. Mol. Catal. A: Chem.* **2000**, *158*, 423. (c) Tsutsui, T.; Kashiwa, N.; Mizuno, A. *Makromol. Chem., Rapid Commun.* **1990**, *11*, 565. (d) Lahelin, M.; Kokko, E.; Lehmus, P.; Pitkänen, P.; Löfgren, B.; Seppälä, J. *Macromol. Chem. Phys.* **2003**, *204*, 1323. (e) Juengling, S.; Muelhaupt, R.; Stehling, U.; Brintzinger, H.-H.; Fischer, D.; Langhauser, F. *J. Polym. Sci., Part A: Polym. Chem.* **1995**, *33*, 1305.

(5) (a) Busico, V.; Cipullo, R.; Chadwick, J. C.; Modder, J. F.; Sudmeijer, O. *Macromolecules* **1994**, *27*, 7538. (b) Busico, V.; Cipullo, R.; Ronca, S. *Macromolecules* **2002**, *35*, 1537. (c) Busico, V.; Cipullo, R.; Talarico, G. *Macromolecules* **1998**, *31*, 2387.

(6) (a) Landis, C. R.; Sillars, D. L.; Batterton, J. M. *J. Am. Chem. Soc.* **2004**, *126*, 8890. (b) Vatamanu, M.; Boden, B. N.; Baird, M. C. *Macromolecules* **2005**, *38*, 9944.

(7) (a) Rieger, B.; Mu, X.; Mallin, D. T.; Rausch, M. D.; Chien, J. C. W. *Macromolecules* **1990**, *23*, 3559. (b) Grassi, A.; Zambelli, A.; Resconi, L.; Albizzati, E.; Mazzocchi, R. *Macromolecules* **1988**, *21*, 617. (c) Stehling, U.; Diebold, J.; Kristen, R.; Röll, W.; Brintzinger, H-. H.; Jüngling, S.; Mülhaupt, R.; Langhauser, F. *Organometallics* **1994**, *13*, 964. (d) Jüngling, S.; Mülhaupt, R.; Stehling, U.; Brintzinger, H-. H.; Fischer, D.; Langhauser, F. *J. Polym. Sci., Part A: Polym. Chem.* **1995**, *33*, 1305.

(8) (a) Song, F.; Cannon, R. D.; Bochmann, M. *J. Am. Chem. Soc.* **2003**, *125*, 7641. (b) Resconi, L.; Camurati, I.; Sudmeijer, O. *Top. Catal.* **1999**, *7*, 145. (c) Resconi, L.; Piemontesi, F.; Camurati, I.; Balboni, D.; Sironi, A.; Moret, M.; Rychlicki, H.; Zeigler, R. *Organometallics* **1996**, *15*, 5046. (d) Dang, V. A.; Yu, L.-C.; Balboni, D.; Dall'Occo, T.; Resconi, L.; Mercandelli, P.; Moret, M.; Sironi, A. *Organometallics* **1999**, *18*, 3781. (e) Resconi, L.; Fait, A.; Piemontesi, F.; Colonnesi, M.; Rychlicki, H.; Zeigler, R. *Macromolecules* **1995**, *28*, 6667.

(9) Liu, Z.; Somsook, E.; White, C. B.; Rosaaen, K. A.; Landis, C. R. *J. Am. Chem. Soc.* **2001**, *123*, 11193.

(10) Busico, V.; Cipullo, R.; Romanelli, V.; Ronca, S.; Togrou, M. *J. Am. Chem. Soc.* **2005**, *127*, 1608.

(11) (a) Bukatov, G. D.; Goncharov, V. S.; Zakharov, V. A. *Macromol. Chem. Phys.* **1995**, *196*, 1751. (b) Spitz, R.; Masson, P.; Bobichon, C.; Guyot, A. *Makromol. Chem.* **1989**, *190*, 717.

(12) Landis, C. R.; Christianson, M. D. *Proc. Natl. Acad. Sci. U.S.A.* **2006**, *103*, 15349.

(13) Al-Humydi, A.; Garrison, J. C.; Mohammed, M.; Youngs, W. J.; Collins, S. *Polyhedron* **2005**, *24*, 1234.

(14) Vatamanu, M.; Stojcevic, G.; Baird, M. C. *J. Am. Chem. Soc.* **2008**, *130*, 454.

(15) (a) Resconi, L. *J. Mol. Catal. A: Chem.* **1999**, *146*, 167. (b) Moscardi, G.; Resconi, L.; Cavallo, L. *Organometallics* **2001**, *20*, 1918.

(16) Karol, F. J.; Kao, S.; Wasserman, E. P.; Brady, R. C. *New J. Chem.* **1997**, *21*, 797.

(17) (a) Jordan, R. F.; LaPointe, R. E.; Bradley, P. K.; Baenziger, N. *Organometallics* **1989**, *8*, 2892. (b) Tjaden, E. B.; Casty, G. L.; Stryker, J. M. *J. Am. Chem. Soc.* **1993**, *115*, 9814.

(18) (a) Horton, A. D. *Organometallics* **1996**, *15*, 2675. (b) Lieber, S.; Prosenc, M.-H.; Brintzinger, H.-H. *Organometallics* **2000**, *19*, 377. (c) Horton, A. D. *Organometallics* **1992**, *11*, 3271.

(19) (a) Yang, X.; Stern, C. L.; Marks, T. J. *J. Am. Chem. Soc.* **1991**, *113*, 3623. (b) Yang, X.; Stern, C. L.; Marks, T. J. *J. Am. Chem. Soc.* **1994**, *116*, 10015.

(20) (a) Samuel, E.; Rausch, M. D. *J. Am. Chem. Soc.* **1973**, *95*, 6263. (b) Hunter, W. E.; Hrncir, D. C.; Bynum, R. V.; Penttila, R. A.; Atwood, J. L. *Organometallics* **1983**, *2*, 750. (c) Massey, A. G.; Park, A. J. *J. Organomet. Chem.* **1964**, *2*, 245.

(21) ^{1}H NMR spectroscopic data of 2,4-dimethyl-1-pentene in C_6D_5Cl, at 25 °C (600 MHz): δ 4.86 (s, CH_2═, 1H), 4.78 (s, CH_2═, 1H), 1.92 (d, $^3J_{HH}$ = 7.6 Hz, CH_2, 2H), 1.77 (m, CH, 1H), 1.71 (s, CH_3, 3H), 0.93 (d, $^3J_{HH}$ = 6.8 Hz, CH_3, 6H) ppm.

(22) (a) A similar ^{1}H NMR *Me*−B resonance of the free $[MeB(C_6F_5)_3]^-$ anion in C_6D_5Cl has been reported by the Jordan group: Carpentier, J.-F.; Wu, Z.; Lee, C. W.; Strömberg, S.; Christopher, J. N.; Jordan, R. F. *J. Am. Chem. Soc.* **2000**, *122*, 7750. (b) For coordination of $[MeB(C_6F_5)_3]^-$ to cationic $[L_2ZrMe]^+$ complexes, see: Jia, L.; Yang, X.; Stern, C. L.; Marks, T. J. *Organometallics* **1997**, *16*, 842.

(23) (a) Silverstein, R. M.; Webster, F. X. *Spectrometric Identification of Organic Compounds*; 6th ed.; Wiley: Chichester, U.K., 1998. (b) Günther, H. *NMR Spectroscopy: Basic Principles, Concepts, and Applications in Chemistry*; 2nd ed.; Wiley: Chichester, U.K., 1995.

(24) (a) Benn, R.; Rufińska, A. *J. Organomet. Chem.* **1982**, *239*, C19. (b) Schlosser, M.; Stähle, M. *Angew. Chem., Int. Ed. Engl.* **1982**, *21*, 145. (c) Brownstein, S.; Bywater, S.; Worsfold, D. J. *J. Organomet. Chem.* **1980**, *199*, 1.

(25) Erker, G.; Berg, K.; Angermund, K.; Krüger, C. *Organometallics* **1987**, *6*, 2620.

(26) Jeske, G.; Lauke, H.; Mauermann, H.; Swepston, P. N.; Schumann, H.; Marks, T. J. *J. Am. Chem. Soc.* **1985**, *107*, 8091.

(27) ^{1}H NMR spectroscopic data of 2,4-dimethyl-1-heptene in C_6D_5Cl at 25 °C (600 MHz): δ 4.87 (s, CH_2═, 1H), 4.81 (s, CH_2═, 1H), 2.07 (dd, J = 6.1 Hz, CH_2, 1H), 1.84 (dd, J = 8.1 Hz, CH_2, 1H), 1.73 (s, CH_3, 3H), 1.65 (m, CH, 1H), 1.40 and 1.32 (2m, CH_2, 2H), 1.33 and 1.11 (2m, CH_2, 2H), 0.96 (t, $^3J_{HH}$ = 7.3 Hz, CH_3, 3H), 0.92 (d, $^3J_{HH}$ = 6.7 Hz, CH_3, 3H) ppm.

(28) Benn, R.; Rufińska, A.; Schroth, G. *J. Organomet. Chem.* **1981**, *217*, 91.

(29) (a) Temme, B.; Erker, G.; Karl, J.; Luftmann, H.; Fröhlich, R.; Kotila, S. *Angew. Chem., Int. Ed. Engl.* **1995**, *34*, 1755. (b) Karl, J.; Erker, G.; Fröhlich, R. *J. Organomet. Chem.* **1997**, *535*, 59. (c) Dahlmann, M.; Erker, G.; Nissinen, M.; Fröhlich, R. *J. Am. Chem. Soc.* **1999**, *121*, 2820. (d) Karl, J.; Erker, G.; Fröhlich, R. *J. Am. Chem. Soc.* **1997**, *119*, 11165.

(30) (a) Abrams, M. B.; Yoder, J. C.; Loeber, C.; Day, M. W.; Bercaw, J. E. *Organometallics* **1999**, *18*, 1389. (b) Benn, R.; Rufińska, A.; Schroth, G. *J. Organomet. Chem.* **1981**, *217*, 91. (c) Faller, J. W.; Incorvia, M. J.; Thomsen, M. E. *J. Am. Chem. Soc.* **1969**, *91*, 518.

(31) (a) Krieger, J. K.; Deutch, J. M.; Whitesides, G. M. *Inorg. Chem.* **1973**, *12*, 1535. (b) Wilke, G.; Bogdanović, B.; Hardt, P.; Heimbach, P.; Keim, W.; Kröner, M.; Oberkirch, W.; Tanaka, K.; Steinrücke, E.; Walter, D.; Zimmermann, H. *Angew. Chem., Int. Ed. Engl.* **1966**, *2*, 151. (c) Becconsall, J. K.; Job, B. E.; O'Brien, S. *J. Chem. Soc. A* **1967**, 423. (d) Faller, J. W.; Thomsen, M. E.; Mattina, M. J. *J. Am. Chem. Soc.* **1971**, *93*, 2642. (e) Cotton, F. A.; Faller, J. W.; Musco, A. *Inorg. Chem.* **1967**, *6*, 179.